Recent Advances in GPS-based Clock Estimation and Steering

Yuriy S. Shmaliy* and Oscar Ibarra-Manzano

Guanajuato University, FIMEE, Ctra. Salamanca-Valle, 3.5+1.8km, Palo Blanco, Salamanca, Gto, Mexico

Abstract: This paper observes recent advances in GPS-based estimation and steering of local clock errors employing the finite impulse response (FIR) technique. The problem we meet here is caused by the GPS time temporary uncertainties and non Gaussian sawtooth noise induces in the commercially available GPS timing receivers. It is connected with the clock nonstationary Gaussian noise with colored (flicker) components often making the Kalman filter low inefficient and requiring weighting averaging. We examine applications of the FIR filtering, prediction, and smoothing solutions for polynomial and state space clock models. Optimal and unbiased FIR estimators are observed in line with the basic and thinning algorithms. The trade-off with the Kalman algorithm is also briefly discussed. It is noticed that, for large averaging horizons featured to highly oversampled and slowly changing with time clock models, simple unbiased FIR solutions become virtually optimal. They seem to be the best choice in terms of simplicity, precision, stability, and robustness in solving many of clock problems in GPS-based timekeeping.

*Address correspondence to these authors at the Guanajuato University, FIMEE, Ctra. Salamanca-Valle, 3.5+1.8km, Palo Blanco, Salamanca, Gto, Mexico

1877-6116/10 2010 Bentham Open

1 Introduction

In our modern life, the function of accurate and precise time dissemination is ordered to the Global Navigation Satellite Systems (GNSS) such as the Global Positioning System (GPS) (USA) [1], Global Navigation System (GLONASS) (Russia), Galileo (Europe), COMPASS (China), and IRNSS (India). The disseminated time signals are used to synchronize time scales in different applications [17, 19, 20, 34, 35]. It is known that precision of the delivered time is limited with noise and temporary time uncertainties caused by different satellites in a view [2]. Therefore, precise correction and prediction of local clock errors cannot usually be achieved directly and optimal estimators are used. The problem with optimal estimation of clock state is also coupled with the clock inherently nonstationary Gaussian noise with colored (flicker) components requiring weighted average solutions. Among possible solutions, the optimal finite impulse response (FIR) estimator seems to be a good choice [21] owing to the following important advantages. Contrary to the infinite impulse response (IIR) recursive structures such as the Kalman filter [12], the transversal FIR structures are inherently bounded input/bounded output (BIBO) stable [13] and have better robustness against temporary uncertainties [11, 8] and round-off errors [13, 14]. Moreover, they allow noise to be nonstationary and colored (flicker) with arbitrary distribution and covariance functions [21].

In this paper, we observe recent advances in GPS-based clock estimation and steering that have been achieved employing FIR estimators [3, 21, 22, 23, 24, 25, 26, 27, 28, 29, 30]. The rest of the paper is organized as follows. In Section 2, we consider a typical measurement set. Time interval errors of the clock are discussed in Section 3. Section 4 gives fundamentals of FIR filtering and discusses problems solved with this technique. Unbiased FIR filtering as well as prediction and smoothing are considered in detail in Sections 5 and 6, respectively. Section 7 is devoted to FIR filtering in state space. Here, we also present possible estimation algorithms. The trade-off with the Kalman filter is outlined in Section 8 and applications are given in Section 9. Finally, concluding remarks are drawn in Section 10.

2 GPS-based Measurement Set

Figure 1 shows a typical measurement set for estimation and steering of local clocks employing the one pulse per second (1PPS) signals of GPS timing receivers [21]. In such receivers, the 1PPS output is generated by the local time clocks (LTCs) referred to the GPS time. To place the latter close to the absolute time, measurements are permanently provided in the United States Naval Observatory (USNO) for the coordinated universal time (UTC) of the USNO master clock (MC). In order to get an estimate of UTC (USNO MC) time derivable from a GPS signal, a set of UTC corrections is provided as part of the message signal. This broadcast message includes the time difference in whole seconds between GPS time and UTC (USNO MC). During 1996, this difference was 11 s [1]. The message also includes the rate and time difference estimate between GPS time and UTC(USNO MC) allowing for a receiver to calculate an accurate estimate of UTC(USNO MC) with the mission goal of 28 ns (1 sigma) [1]. Outside the selective availability (SA) induced for security purposes, the estimate may have an accuracy of about 10 ns in the root mean squares sense. Practically, the USNO has been successful in predicting UTC to within about 10 ns [1]. A real-time potential uncertainty of GPS time for UTC (USNO MC) stays therefore at a level of about 14-ns [1]. The standard deviation of GPS time available precision mostly depends on random errors in different onboard clocks and different satellites in a view. It can be achieved at a level of 3-5 ns [16, 18].

To obtain high accuracy, all time delays featured to channels and signal propagation are compensated at the early stage. The main source of random errors that cannot be removed from the received signal below 3–5 ns [16, 18] is associated with the GPS time precision (b) limited by different satellites in a view at their nonstationary orbits. The receiver adds the sawtooth noise (c) bounded with $\pm\Delta$, where $\Delta[\text{ns}] = \frac{10^3}{2f_{\text{LTC}}[\text{MHz}]}$ and f_{LTC} is the frequency of the LTC oscillator. In the receivers such as the SynPaQ III GPS Sensor, this frequency is chosen to be 10 MHz and the bound is thus $\Delta = 50$ ns.

Contrary to the error 1 PPS signal (d) that is zero-mean with uncertainty (b) and sawtooth noise (c), the time interval error (TIE) (e) of a local clock is inherently nonstationary and random, although having low intensity short-time noise. If a high resolution time interval counter is used, then the difference between (e) and (d) represents the local clock measured TIE. The latter has the form (f) or (g) if measurement is provided with and without sawtooth (using the negative sawtooth code supplied by the receiver), respectively. To smooth excursions and eliminate sawtooth in an optimum way, a digital estimator (Filter) of the clock TIE is used. If the filter is optimal or close to optimal in the minimum mean square error (MSE) sense, then its output (h) ranges most closely to the actual behavior (e) and the TIE of a locked clock becomes near stationary (i) with a small amount of random departures.

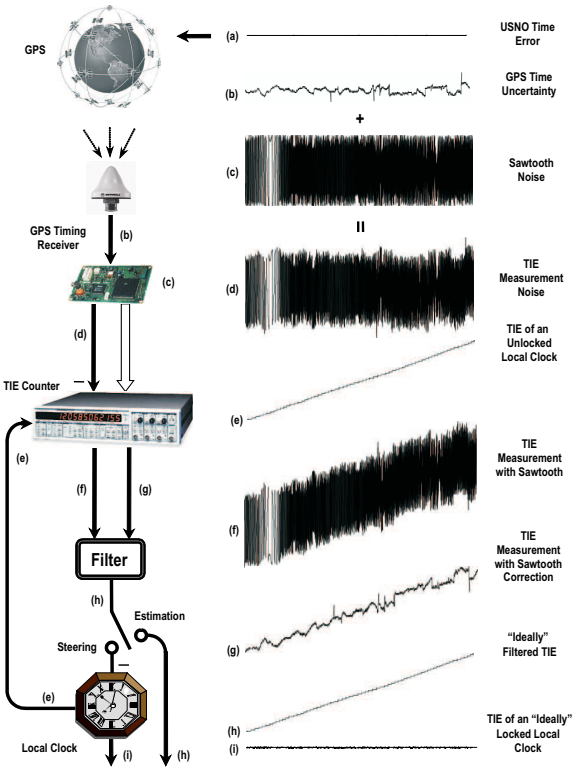

Figure 1: A typical set for GPS-based measurement, estimation, and steering of clock errors [21].

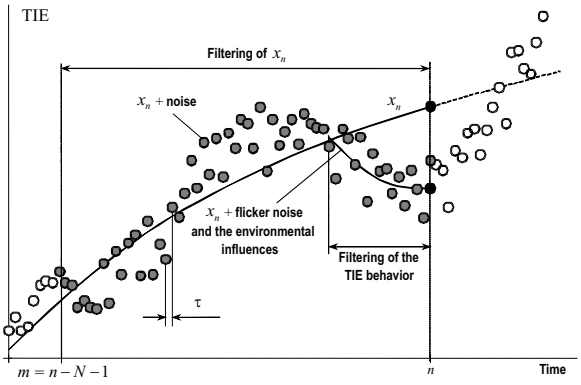

Figure 2: FIR filtering of x_n on a horizon of N points.

3 Clock TIE

Any clock has the time difference (TIE [5]) for an ideal uniform time scale. The TIE can be modeled in continuous time t using the finite Taylor series as [6]

$$x(t) = x(0) + y(0)t + \frac{z(0)}{2}t^2 + w_{\mathrm{PM}}(t) + \int_0^t w_{\mathrm{FM}}(\theta)\mathrm{d}\theta\,, \tag{1}$$

where $x(0)$ is the initial TIE, $y(0)$ is the fractional frequency offset at zero of a local clock oscillator, $z(0)$ is the linear frequency drift rate at zero, $w_{\mathrm{PM}}(t)$ is the phase noise, and $w_{\mathrm{FM}}(t)$ is the frequency noise. The IEEE Standard [5] suggests that the three state clock model such as (1) serves on an infinite time interval and that the higher order states are included to the random part.

The TIE is measured over a time interval τ starting at $t - \tau$ and ending at t. Thus, (1) can be represented in discrete time n with digital numbers x_n as

$$x_n = x_0 + y_0\tau n + \frac{z_0}{2}\tau^2 n^2 + w_{\mathrm{PM}n} + \tau\sum_{i=0}^{n} w_{\mathrm{FM}i}\,, \tag{2}$$

where $x_0 = x(0)$, $y_0 = y(0)$, and $z_0 = z(0)$. In precise clocks, y_0 and z_0 are extremely small and the deterministic part in (2) is slowly changing with time. On the other hand, both $w_{\mathrm{PM}n}$ and $w_{\mathrm{FM}n}$ contain fast white and slow colored (flicker and random walk) Gaussian components. For $w_{\mathrm{FM}i}$ white, the last term in (2) represents the discrete-time Wiener process, making (2) near Markovian in the presence of phase noise and the environmental influences (Fig. 2). Owing to such features of the process, the clock estimation problems have some specifics:

- Short base of $10^2 \ldots 10^3$ s is employed for synchronizing the crystal and rubidium clocks. Here the slow noise components are commonly tracked and the white phase noise is filtered out.

- Long base of about 10^5 s is required for filtering and prediction in atomic clocks. Maximum accuracy is achieved here if most of the noise components and the environmental effects are filtered out.
- A very long base of 10^7 s is processed in order to estimate the Allan variance.
- All the data available is used in order to estimate the current clock state.

4 FIR Estimation of Clock Errors

The TIE measurement s_n is commonly considered as an additive sum of the TIE x_n and zero-mean, $E\{v_n\} = 0$, measurement noise v_n,

$$s_n = x_n + v_n \,, \tag{3}$$

where noise is supposed to be negligible in direct measurement and can be large when the reference time is remotely delivered by the commercially available receivers of wireless GNSS systems.

The FIR filtering estimate $\hat{x}_n$ of x_n is the weighted average of s_n over $N \geqslant 2$ points via the discrete convolution of s_n and the FIR filter gain (impulse response) $h_{ln} \triangleq h_{ln}(N)$, where l is the degree of the gain [26]. This estimate can thus be represented in the following equal forms of

$$\hat{x}_n = \sum_{i=0}^{N-1} h_{li} s_{n-i} \tag{4}$$

$$= \mathbf{W}_l^T \mathbf{S}_N = \mathbf{S}_N^T \mathbf{W}_l \,, \tag{5}$$

where the $N \times 1$ measurement vector and the $N \times 1$ filter gain matrix are specified with, respectively,

$$\mathbf{S}_N = [s_n \, s_{n-1} \, \ldots, s_{n-N+1}]^T \,, \tag{6}$$

$$\mathbf{W}_l = [h_{l0} \, h_{l1} \, \ldots, h_{l(N-1)}]^T \,. \tag{7}$$

Note that there always exists some error $\epsilon_n = x_n - \hat{x}_n$ to be minimized in some sense, by optimizing h_{ln} or $\mathbf{W}_l$. The minimum MSE sense is commonly used, albeit it is not always appropriate for all clock applications.

4.1 Problems Solved with FIR Structures

The following clock estimation problems can be solved employing the FIR structures.

- Filtering is commonly used in timescales to estimate the present state [7, 22, 23, 24, 25, 26, 30, 31]. To enable, a nearest past history can be processed from $n - N + 1$ to n and the estimate related to n, by (4) or (5).

- Prediction is employed to evaluate possible future errors in time scales [7]. A 1-step prediction is used in clock steering [3] and the p-step one is a key solution for holdover [6, 27, 28], when a synchronizing signal is temporary not available. The p-step prediction at $n+p$, $p>0$, is provided with

$$\tilde{x}_{n+p} = \sum_{i=0}^{N-1} \tilde{h}_{li}(p) s_{n-i}\,, \quad p>0\,, \tag{8}$$

where $\tilde{h}_{ln}(p) \triangleq \tilde{h}_{ln}(N,p)$ is the p-dependent gain defined in [21]. The predictive FIR filtering estimate is obtained at n via the past history from $n-N+1-p$ to $n-p$ as

$$\tilde{x}_{n} = \sum_{i=p}^{N-1+p} h_{li}(p) s_{n-i}\,, \quad p>0\,, \tag{9}$$

where $h_{ln}(p) \triangleq h_{ln}(N,p)$ is the gain defined in [28].

- Smoothing is used for noise reduction in postprocessing, identification of clock models, and ascertaining the initial clock state for optimal algorithms. In this regard, FIR smoothing can be organized to have a fixed lag (p is constant), fixed interval (N is constant), or fixed point ($n-p$ is constant). The FIR smoother and the smoothing FIR filter are designed as follows, respectively,

$$\bar{x}_{n+p} = \sum_{i=0}^{N-1} \tilde{h}_{li}(p) s_{n-i}\,, \quad p<0\,, \tag{10}$$

$$\bar{x}_{n} = \sum_{i=p}^{N-1+p} h_{li}(p) s_{n-i}\,, \quad p<0\,. \tag{11}$$

As can be seen, the difference between (8) and (10) as well as between (9) and (11) exists only in the sign of p and that, by $p=0$, (8)–(11) become (4).

The gains $h_{ln}(p)$ and $\tilde{h}_{ln}(p)$ in (8)–(11) are coupled as $\tilde{h}_{ln}(p) = h_{l(n+p)}(p)$. Note that the estimates (4) and (8)–(11) have practical usefulness only if the gains are specified and optimized in some sense. The most common ways of the optimization are the following.

5 Unbiased FIR Filtering of the TIE

The unbiased FIR filtering estimate is optimal in the zero-bias sense. The relevant unbiased gain h_{ln} can be found from the unbiasedness condition [33]

$$E\{x_n\} = E\{\hat{x}_n\}\,, \tag{12}$$

meaning that the average of the estimate is required to be equal to that of its origin. Substituting (3) to (4) and then averaging both sides of (4), by (12), gives us

$$x_n = \sum_{i=0}^{N-1} h_{li} x_{n-i} \tag{13}$$

Further substituting the determinist part of (2) to (13) leads to the fundamental properties of the unbiased FIR filters [22]:

$$\sum_{i=0}^{N-1} h_{li} = 1\,, \tag{14}$$

$$\sum_{i=0}^{N-1} h_{li} i^u = 0\,, \quad 1 \leqslant u \leqslant l\,, \tag{15}$$

which can be rewritten in a short matrix form as [22]

$$\bar{\mathbf{W}}_l^T \mathbf{V} = \mathbf{J}^T\,, \tag{16}$$

where $\mathbf{J} = [1\,0\,\ldots\,0]^T$, $\bar{\mathbf{W}}_l^T$ is given by (6), and $\mathbf{V}$ is the Vandermonde matrix, specified below for arbitrary l as

$$\mathbf{V} = \begin{bmatrix} 1 & 0 & 0 & \ldots & 0 \\ 1 & 1 & 1 & \ldots & 1 \\ 1 & 2 & 2^2 & \ldots & 2^l \\ \vdots & \vdots & \vdots & \ddots & \vdots \\ 1 & N-1 & (N-1)^2 & \ldots & (N-1)^l \end{bmatrix}. \tag{17}$$

A solution to (16) has the form of [22, 36]

$$\bar{\mathbf{W}}_l^T = \mathbf{J}^T (\mathbf{V}^T \mathbf{V})^{-1} \mathbf{V}^T\,, \tag{18}$$

representing the first row of the minimum variance unbiased (MVU) estimator [33], in which the observation matrix is Vandermonde (18).

5.1 Polynomial FIR Filter Gain

Further development of (18) has been provided in [22] exploiting what is knows from the Kalman filter theory [12]: the order of the optimal filter is the same as that of the system. Hence, the m-degree TIE polynomial function x_n can unbiasedly be filtered if the polynomial gain h_{lp} has the same degree $l = m$. Note that unbiasedness is also achieved if $l > m$, although with larger noise [22]. Referring to this fact, h_{ln} can be substituted with

$$h_{ln} = \sum_{j=0}^{l} a_{jl} n^j\,, \tag{19}$$

where the generic coefficient a_{jl} is defined as

$$a_{jl} = (-1)^j \frac{M_{(j+1)1}}{|\mathbf{D}|} \tag{20}$$

via the determinant $|\mathbf{D}|$ and minor $M_{(j+1)1}$ of a short $(l+1)\times(l+1)$ quadratic symmetric matrix [22, 36]

$$\mathbf{D} = \mathbf{V}^T\mathbf{V} = \begin{bmatrix} d_0 & d_1 & \dots & d_l \\ d_1 & d_2 & \dots & d_{l+1} \\ \vdots & \vdots & \ddots & \vdots \\ d_l & d_{l+1} & \dots & d_{2l} \end{bmatrix}, \tag{21}$$

which component d_r, $r \in [0, 2l]$, is calculated using the Bernoulli polynomials $B_n(x)$ as

$$d_r(N) = \sum_{i=0}^{N-1} i^r = \frac{1}{r+1}\left[B_{r+1}(N) - B_{r+1}\right]. \tag{22}$$

By (20)–(22), h_{ln} can be found for any l, although, following [5], only low-degree gains are exploited in solving clock problems.

5.1.1 Low-degree Polynomial Gains

For low-state clock models [5], the unique polynomial gains have been found in [22] to be

$$h_{0n} = \frac{1}{N}, \tag{23}$$

$$h_{1n} = \frac{2(2N-1)-6n}{N(N+1)}, \tag{24}$$

$$h_{2n} = \frac{3(3N^2-3N+2)-18(2N-1)n+30n^2}{N(N+1)(N+2)}, \tag{25}$$

$$h_{3n} = \frac{8(2N^3-3N^2+7N-3)-20(6N^2-6N+5)n}{N(N+1)(N+2)(N+3)} + \frac{120(2N-1)n^2-140n^3}{N(N+1)(N+2)(N+3)}. \tag{26}$$

The gain (23) represents simple averaging widely used in atomic clocks for noise reduction. The ramp gain (24) was originally derived in [23] via linear regression, once the latter is used to model systematic behaviors in clocks [5]. Figure 3 illustrates these gains graphically and their applications in GPS-based timekeeping can be found in [22, 23, 24, 26, 30].

5.1.2 Noise Power Gain

Following [9], noise amount in the unbiased FIR filter output can be estimated with the noise power gain (NPG) $g_l = \sigma_x^2/\sigma_v^2$, where σ_v^2 is the variance of the

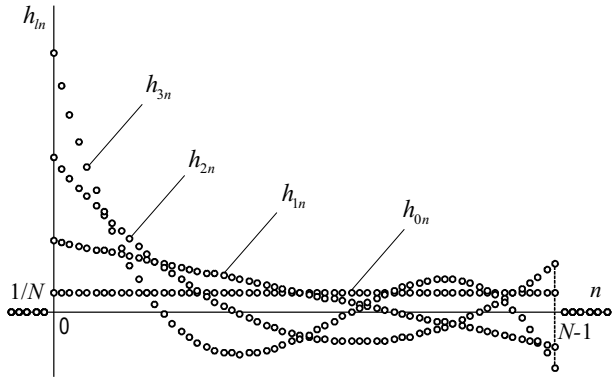

Figure 3: Low-degree unique unbiased FIR filter gains.

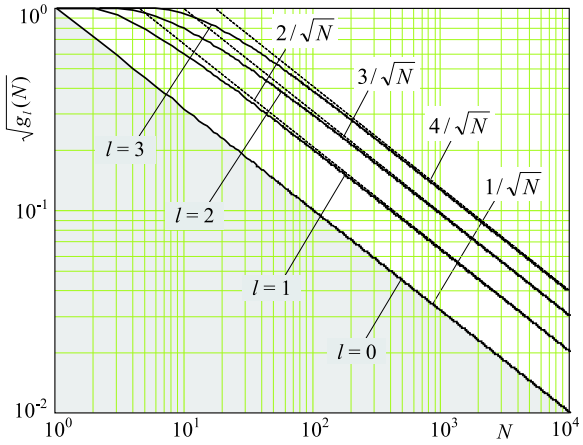

Figure 4: The NPGs of the low-degree unbiased FIR filters.

delta-correlated measurement noise v_n and σ_x^2 is the variance of the estimate. The NPG can also be evaluated via the gain h_{ln} as [9, 27]

$$g_l = \sum_{i=0}^{N-1} h_{li}^2 = \mathbf{W}_l^T \mathbf{W}_l = a_{0l} \,. \tag{27}$$

As can be seen, diminishing noise means reducing a_{0l} in (19) by increasing N.

Figure 4 sketches g_l for the low-degree unbiased FIR filters. A shadowed area is a dead zone that theoretically can never be reached. Its bound is depicted by $1/\sqrt{N}$ associated with simple averaging with the gain (23) producing noise minimum among all other filters [32]. It has been shown in [22] that, if $l > 0$, the function $\sqrt{g_l(N)}$ traces above the lower bound $1/\sqrt{N}$ and below the upper

bound as

$$\frac{1}{\sqrt{N}} < \sqrt{g_l(N)} < \begin{cases} \frac{l+1}{\sqrt{N}}, & N \geqslant (l+1)^2 \\ 1, & N < (l+1)^2 \end{cases}, \quad l > 0\,. \tag{28}$$

5.1.3 Optimal τ and N

Although the IEEE Standard [5] suggests that the clock has three states, the m-degree polynomial can be applied in order to filter out measurement noise. It follows from Fig. 2 that the l-degree gain fits the clock model only on a finite horizon of N points, when $l \geqslant m$. If $l < m$, bias occurs in the estimate and N is thus limited with the minimum MSE. Because N depends on the sampling time τ, the MSE must also be minimized by searching for a proper τ.

In GPS-based timekeeping via 1PPS signals, $\tau_{\rm opt}$ is 1 s [24]. In turn, $N_{\rm opt}$ for simple averaging (23) and ramp gain (24) are determined in [24] by, respectively,

$$N_{\rm opt}(l=0) = \left\lfloor \sqrt[3]{\frac{2\sigma_v^2}{\tau^2 y^2}} \right\rfloor, \tag{29}$$

$$N_{\rm opt}(l=1) = \left\lfloor \sqrt[5]{\frac{144\sigma_v^2}{\tau^4 z^2}} \right\rfloor, \tag{30}$$

where $\lfloor a \rfloor$ means an integer part of a. If y_n and z_n are not available at n, one can substitute them with the maximum values featured to particular clocks. Then (29) and (30) would serve as lower bounds for $N_{\rm opt}$.

5.1.4 Optimal Ramp Gain

A modification of the ramp gain to be optimum in the minimum MSE sense was provided in [26] in the form of

$$h_{1n}(\eta) = \frac{1}{N}\left[1 + \eta\frac{3(N-1)-6n}{N+1}\right], \tag{31}$$

where η is an optimization coefficient. As can be seen, (31) becomes (24), if $\eta = 1$, and $\eta = 0$ simplifies it to (23). The optimal value of η_0, $0 < \eta_0 < 1$, was specified in [26] in the minimum MSE sense as

$$\eta_0 = \frac{\alpha^2 N(N^2-1)}{\alpha^2 N(N^2-1)+12} \tag{32}$$

with $\alpha^2 = \tau^2 y^2/\sigma_v^2$. It has also been shown in [26] that, for crystal, rubidium, and cesium clocks, η_0 ranges as, respectively,

$$\begin{aligned} 0.992124198176391 &< \eta_0 < 0.999999999964719\,, \\ 0.998451946589028 &< \eta_0 < 0.999999993798186\,, \\ 0.969923570257806 &< \eta_0 < 0.999950387946414\,, \end{aligned}$$

meaning that η_0 takes values very closely related to unity. The unbiased and optimal estimates are thus indistinguishable and there would be no reasonable necessity in using optimal filters to solve many of the clock problems. Note that (31) requires four coefficients, τ, y, σ_v^2, and N, whereas (24) needs only N.

6 Unbiased FIR Prediction and Smoothing

It follows from (8)–(11) that prediction and smoothing are provided by the same convolution batch if to let p be either positive or negative, respectively.

To organize unbiased predictive FIR filtering (9), by $p > 0$, or smoothing FIR filtering (11), by $p < 0$, the Vandermonde matrix was modified in [21] to

$$\mathbf{V}(p) = \begin{bmatrix} 1 & p & \dots & p^l \\ 1 & p+1 & \dots & (p+1)^l \\ 1 & p+2 & \dots & (p+2)^l \\ \vdots & \vdots & \ddots & \vdots \\ 1 & N-1+p & \dots & (N-1+p)^l \end{bmatrix}, \tag{33}$$

obeying the following fundamental properties of the unbiased gain, existing from p to $p+N-1$:

$$\sum_{i=p}^{N-1+p} h_{li}(p) = 1 \tag{34}$$

$$\sum_{i=p}^{N-1+p} h_{li}(p) i^u = 0\,, \quad 1 \leqslant u \leqslant l\,. \tag{35}$$

With $\mathbf{V}(p)$ specified by (33), the gain $h_{li}(p)$ can serve to provide prediction and smoothing.

Substituted (33) to (22), the p-dependent components of the matrix $\mathbf{D}(p)$ is specified via the Bernoulli polynomials with [28]

$$d_r(N,p) = \sum_{i=p}^{N-1+p} i^r = \frac{B_{r+1}(N+p) - B_{r+1}(p)}{r+1}\,. \tag{36}$$

Provided $\mathbf{D}(p)$, the p-dependent gain $h_{ln}(p)$ can also be found analytically for any l and p. Below we consider only the p-step predictive ramp FIR filter, noticing that a quadratic solution can be found in [21, 28].

6.1 The p-step Predictive Ramp FIR Filter

The gain of the p-step ramp predictive FIR filter has a familiar form of

$$h_{1n}(p) = a_{01}(p) + a_{11}(p)n \tag{37}$$

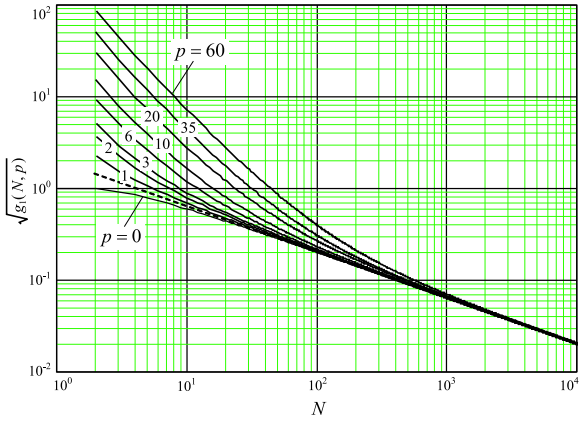

Figure 5: The NPG of the p-step predictive unbiased ramp FIR filter.

with the p-dependent coefficients found in [27, 28] to be

$$a_{01}(p) = \frac{2(2N-1)(N-1)+12p(N-1+p)}{N(N^2-1)}, \quad (38)$$

$$a_{11}(p) = -\frac{6(N-1+2p)}{N(N^2-1)}. \quad (39)$$

The NPG for this gain is $g_1(p) = a_{01}(p)$ (38). By $p = 0$, (37) becomes (24). For $p = 1$, function (37) was originally derived and investigated in [9] using the Lagrange multipliers. An analysis reveals that an increase in p results in a higher slope of $h_{1n}(p)$ as well as in an increase on $6p/N(N+1)$ in both positive and negative peak values.

A payment for prediction is instability. In fact, both (38) and (39) tend toward infinite if $N \to 1$ that makes prediction inefficient when $g_l(p)$ exceeds unity (noise is not attenuated) with small N. The latter is neatly seen in Fig. 5. On the other hand, with $N \gg 1$, the filter is highly efficient and its NPG fits an asymptotic $g_l \cong 4/N$ (dashed in Fig. 5) that does not depend on p.

Figure 6 gives us an idea of how well the ramp FIR predictor works, covering the range of about 0.5 hours via the GPS-based measurements of the TIE [27]. As can be seen, $\tilde{x}_n$ inherently diverges in the holdover range, when measurement is not temporary available, and then converges to x_n in the hold-in range. Different prediction algorithms with examples of applications for such measurements can be found in [27, 28].

7 FIR Filtering in State Space

In line with the polynomial model (2), clock representation in state space is also widely used. It has been proposed in [2], to represent the clock in state space

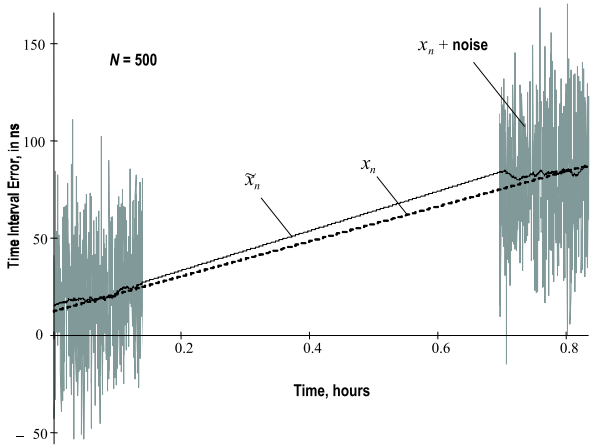

Figure 6: Prediction of clock errors with a ramp unbiased FIR filter in the presence of large measurement noise.

with the state and observation equations, respectively,

$$\mathbf{x}_n = \mathbf{A}\mathbf{x}_{n-1} + \mathbf{w}_n \,, \tag{40}$$

$$s_n = \mathbf{C}\mathbf{x}_n + v_n \,, \tag{41}$$

where the 3×1 state vector is given by

$$\mathbf{x}_n = [x_n \, y_n \, z_n]^T \,, \tag{42}$$

the 3×3 clock matrix

$$\mathbf{A} = \begin{bmatrix} 1 & \tau & \frac{\tau^2}{2} \\ 0 & 1 & \tau \\ 0 & 0 & 1 \end{bmatrix} \tag{43}$$

projects the nearest past state $\mathbf{x}_{n-1}$ to the present state $\mathbf{x}_n$ via the finite Taylor series expansions, and the 1×3 observation matrix is $\mathbf{C} = [\,1\,0\,0\,]$.

The 3×1 vector of the clock zero-mean noises,

$$\mathbf{w}_n = [w_{xn} \, w_{yn} \, w_{zn}]^T \,, \tag{44}$$

has the covariance matrix $\mathbf{\Psi} = E\{\mathbf{w}_i \mathbf{w}_j^T\}$, which components are specified via the noise power laws determined in [5]. As shown in [4], the following matrix can be used for the white Gaussian approximation of $\mathbf{\Psi}$,

$$\bar{\mathbf{\Psi}} = \tau \begin{bmatrix} q_1 + \frac{q_2\tau^2}{3} + \frac{q_3\tau^4}{20} & \frac{q_2\tau}{2} + \frac{q_3\tau^3}{8} & \frac{q_3\tau^2}{6} \\ \frac{q_2\tau}{2} + \frac{q_3\tau^3}{8} & q_2 + \frac{q_3\tau^2}{3} & \frac{q_3\tau}{2} \\ \frac{q_3\tau^2}{6} & \frac{q_3\tau}{2} & q_3 \end{bmatrix} \,, \tag{45}$$

where the diffusion coefficients q_1, q_2, and q_3 specify the white FM noise (WHFM), white random walk FM noise (WRFM), and white random run FM noise (RRFM), respectively, in the τ-domain power law [5] of the clock's oscillator.

The noise v_n associated with GPS-based measurement is zero-mean, $E\{v_n\} = 0$. It has the variance $E\{v_n^2\} = \sigma_v^2$ and supposedly arbitrary distribution and covariance. An analysis of this noise can be found in [21].

7.1 Representation on the Averaging Horizon

To apply FIR filtering to the clock state space model, (40) and (41), the latter is represented in [21] on a horizon of N point from $m = n - N + 1$ to n (Fig. 2) as

$$\mathbf{X}_{n,m} = \mathbf{A}_{n-m}\mathbf{x}_m + \mathbf{B}_{n-m}\mathbf{N}_{n,m}\,, \tag{46}$$

$$\mathbf{S}_{n,m} = \mathbf{C}_{n-m}\mathbf{x}_m + \mathbf{G}_{n-m}\mathbf{N}_{n,m} + \mathbf{V}_{n,m}\,, \tag{47}$$

where

$$\mathbf{X}_{n,m} = \left[\mathbf{x}_n^T\, \mathbf{x}_{n-1}^T \ldots \mathbf{x}_m^T\right]^T\,, \tag{48}$$

$$\mathbf{S}_{n,m} = \left[s_n\, s_{n-1} \ldots s_m\right]^T\,, \tag{49}$$

$$\mathbf{N}_{n,m} = \left[\mathbf{w}_n^T\, \mathbf{w}_{n-1}^T \ldots \mathbf{w}_m^T\right]^T\,, \tag{50}$$

$$\mathbf{V}_{n,m} = \left[v_n\, v_{n-1} \ldots v_m\right]^T, \tag{51}$$

$$\mathbf{A}_i = \left[(\mathbf{A}^i)^T\, (\mathbf{A}^{i-1})^T \ldots \mathbf{A}^T\, \mathrm{I}\right]^T\,, \tag{52}$$

$$\mathbf{A}^i = \begin{bmatrix} 1 & \tau i & \frac{(\tau i)^2}{2} \\ 0 & 1 & \tau i \\ 0 & 0 & 1 \end{bmatrix}, \tag{53}$$

$$\mathbf{B}_i = \begin{bmatrix} \mathbf{A}^0 & \mathbf{A} & \ldots & \mathbf{A}^{i-1} & \mathbf{A}^i \\ \mathbf{0} & \mathbf{A}^0 & \ldots & \mathbf{A}^{i-2} & \mathbf{A}^{i-1} \\ \vdots & \vdots & \ddots & \vdots & \vdots \\ \mathbf{0} & \mathbf{0} & \ldots & \mathbf{A}^0 & \mathbf{A} \\ \mathbf{0} & \mathbf{0} & \ldots & \mathbf{0} & \mathbf{A}^0 \end{bmatrix}, \tag{54}$$

$$\mathbf{C}_i = \left[\begin{array}{cccccc} (\mathbf{A}^i)_1^T & (\mathbf{A}^{i-1})_1^T & \ldots & (\mathbf{A}^1)_1^T & (\mathbf{A}^0)_1^T \end{array}\right]^T, \tag{55}$$

$$(\mathbf{A}^i)_1 = \left[\begin{array}{ccc} 1 & \tau i & (\tau i)^2/2 \end{array}\right], \tag{56}$$

$$\mathbf{G}_i = \begin{bmatrix} (\mathbf{I})_1 & (\mathbf{A})_1 & \ldots & (\mathbf{A}^{i-1})_1 & (\mathbf{A}^i)_1 \\ \mathbf{0} & (\mathbf{I})_1 & \ldots & (\mathbf{A}^{i-2})_1 & (\mathbf{A}^{i-1})_1 \\ \vdots & \vdots & \ddots & \vdots & \vdots \\ \mathbf{0} & \mathbf{0} & \ldots & (\mathbf{I})_1 & (\mathbf{A})_1 \\ \mathbf{0} & \mathbf{0} & \ldots & \mathbf{0} & (\mathbf{I})_1 \end{bmatrix}, \tag{57}$$

where $(\mathbf{Z})_1$ means the first row of a matrix $\mathbf{Z}$ and $\mathbf{0}$ is a relevant matrix with all components equal to zero. Note that the initial state $\mathbf{x}_m$ is supposed to be

given exactly, although it is randomly valued. Therefore, $\mathbf{w}_m$ is always zero valued.

By this model, the slowly changing clock states are represented at n with the finite Taylor series expansions via the states at m as follows:

$$\begin{aligned} x_n &= x_m + (n-m)\tau y_m \\ &\quad + \frac{(n-m)^2\tau^2 z_m}{2} + w_{xn}\,, \qquad (58) \\ y_n &= y_m + (n-m)\tau z_m + w_{yn}\,, \qquad (59) \\ z_n &= z_m + w_{zn}\,, \qquad (60) \end{aligned}$$

where w_{xn}, w_{yn}, and w_{zn} conventionally represent the noise components on the averaging horizon.

7.2 Optimal FIR Filtering of the TIE

Utilizing N measurement points from $n-N+1$ to n, the FIR filtering estimate $\hat{x}_n$ of x_n is obtained, by (5) applied to (47), as

$$\hat{x}_n = \mathbf{W}_l^T \mathbf{S}_{n,m}\,. \qquad (61)$$

In order for the estimate (61) to be optimal, the degree of the gain must be set such that $l = K - k$, where K is a number of the states and k is the filtered state [22]. For the 3-state clock model and filtered first state, one thus sets $l = 2$.

The optimal gain matrix $\tilde{\mathbf{W}}_l$ for (61) was specified in [25, 29] as

$$\tilde{\mathbf{W}}_l^T = (\mathbf{A}^{N-1})_1 \mathbf{R}_m \mathbf{C}_{n-m}^T (\mathbf{Z}_m + \tilde{\mathbf{Z}}_\Psi + \mathbf{\Phi}_V)^{-1}\,, \qquad (62)$$

where

$$\begin{aligned} \mathbf{Z}_m &= \mathbf{C}_{n-m}\mathbf{R}_m\mathbf{C}_{n-m}^T\,, \qquad (63) \\ \tilde{\mathbf{Z}}_\Psi &= \mathbf{G}_{n-m}\mathbf{\Psi}_N\mathbf{G}_{n-m}^T\,. \qquad (64) \end{aligned}$$

The noise covariance function matrices are

$$\begin{aligned} \mathbf{\Psi}_N &= E\{\mathbf{N}_{n,m}\mathbf{N}_{n,m}^T\}\,, \qquad (65) \\ \mathbf{\Phi}_V &= E\{\mathbf{V}_{n,m}\mathbf{V}_{n,m}^T\} \qquad (66) \end{aligned}$$

and the initial state covariance is

$$\mathbf{R}_m = E\{\mathbf{x}_m\mathbf{x}_m^T\}\,. \qquad (67)$$

It has been shown in [21] that the initial state function $\mathbf{Z}_m$ can *a posteriori* be determined in the filter algorithm by solving the discrete algebraic Riccati equation.

Although (62) can be applied to the state space models with different kinds of noise sources (unlike the Kalman filter claiming all noises to be white sequences), it presumes large computational burden when N is large. Following [25], substantial simplifications of (62) can be achieved for $N \gg 1$ associated with GPS-based timekeeping and precision clocks.

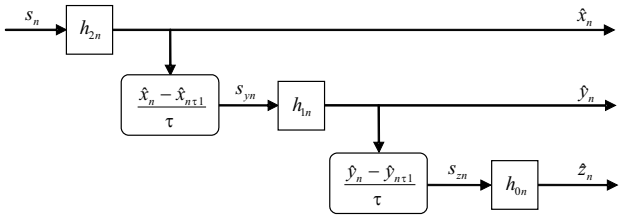

Figure 7: The basic FIR filtering algorithm for TIE measurements of the 3-state clock model.

7.2.1 Large Averaging Horizon, $N \gg 1$

When $N \gg 1$ or the initial mean square state dominates noise in order of magnitudes, the second and third terms can be neglected in the parenthesis of (62) [25]. Accordingly, (62) first reduces to

$$\tilde{\mathbf{W}}_l^T = (\mathbf{A}^{N-1})_1 \mathbf{R}_m \mathbf{C}_{n-m}^T (\mathbf{C}_{n-m} \mathbf{R}_m \mathbf{C}_{n-m}^T)^{-1} . \tag{68}$$

and, following [21], can be transformed to the unbiasedness (or deadbeat [13]) constraint

$$\tilde{\mathbf{W}}_l^T \mathbf{C}_{n-m} = (\mathbf{A}^{N-1})_1 , \tag{69}$$

where the gain $\tilde{\mathbf{W}}_l$ is exactly that specified with (19) [22]. Provided large N, the optimal estimate of the clock TIE is thus obtained with the unbiased FIR filter (see an experimental verification given in [26]).

8 FIR Filtering Algorithms

An important special feature of FIR filtering is that it can be applied to each of the states separately [13, 22]. Although, so far, we discussed the estimates of the clock first state x_n, the remaining states can be estimated similarly [22], even with the individual optimal horizons and sampling intervals [24, 30]. The clock states can also be estimated all at once as shown in [21].

8.1 Basic Algorithm

The basic unbiased FIR filtering algorithm for the most common 3-state clock model is shown in Fig. 7 [22]. Here, the quadratic gain (25) is used to produce the estimate $\hat{x}_n$ of the TIE (Fig. 8) via the convolution (4). The noise variance in the produced estimate is approximately evaluated by the NPG $g_2 = a_{02}$.

Because the fractional frequency offset can be specified by the discrete-time derivative of the TIE, the measurement of y_n is formed as $s_{yn} = (\hat{x}_n - \hat{x}_{n-1})/\tau$. Then the FIR filter with the ramp gain (24) is applied to produce the estimate $\hat{y}_n$ with the variance calculated by the NPG $g_1 = a_{01}$. The procedure is repeated using simple averaging (23) applied to the derivative $s_{zn} = (\hat{y}_n - \hat{y}_{n-1})/\tau$ in

order to obtain an estimate $\hat{z}_n$ of the linear frequency drift rate z_n with the error approximately calculated by the NPG $g_0 = 1/N$.

For the 3-state and 2-state clock models, the unbiased FIR filtering batch algorithms are hence as in the following.

3-state clock model. If the clock is identified to have three states, FIR filtering obtains

$$\hat{x}_n = \sum_{i=0}^{N_x-1} h_{2i} s_{n-i}\,, \tag{70}$$

$$\hat{y}_n = \frac{1}{\tau} \sum_{j=0}^{N_y-1} h_{1j} [\hat{x}_{n-j} - \hat{x}_{n-j-1}]\,, \tag{71}$$

$$\hat{z}_n = \frac{1}{\tau N_z} \sum_{r=0}^{N_z-1} [\hat{y}_{n-r} - \hat{y}_{n-r-1}]\,, \tag{72}$$

where the averaging horizons N_x, N_y, and N_z are typically different. The first accurate value of $\hat{x}_n$ appears at $N_x - 1$, of $\hat{y}_n$ at $N_x + N_y - 1$, and of $\hat{z}_n$ at $N_x + N_y + N_z - 1$.

2-state clock model. For the 2-state clock model, the existing states are filtered by

$$\hat{x}_n = \sum_{i=0}^{N_x-1} h_{1i} s_{n-i}\,, \tag{73}$$

$$\hat{y}_n = \frac{1}{\tau N_y} \sum_{j=0}^{N_y-1} (\hat{x}_{n-j} - \hat{x}_{n-j-1})\,. \tag{74}$$

Here, the first accurate value of $\hat{x}_n$ appears at $N_x - 1$ and of $\hat{y}_n$ at $N_x + N_y - 1$.

8.2 Thinning Algorithm

Following [24], the optimal step $\tau_{x\text{opt}}$ is 1 s for the first clock state in GPS-based measurements via the 1 PPS signals. In contrast, $\tau_{y\text{opt}}$ and $\tau_{z\text{opt}}$ must be set individually for the second and third states [24].

An improved "thinning" algorithm has been proposed in [30] with the diagram shown in Fig. 8. This algorithm accounts for the individual τ_y and τ_z, implied that the thinning coefficients, k_y and k_z, are chosen such that information is not lost about the states.

It follows from Fig. 8 that the first state x_n is estimated by (70) as $\hat{x}_n$ and that this estimate is then thinned out by changing τ to $\tau_y = k_y\tau$. In a new discrete scale $m_y = \left\lfloor \frac{n}{k_y} \right\rfloor$, where $\lfloor \frac{a}{b} \rfloor$ represents an integer part of the ratio, the estimate becomes $\hat{x}_{k_y m_y}$. Then the one pulse per k_y seconds (1PPk_yS)

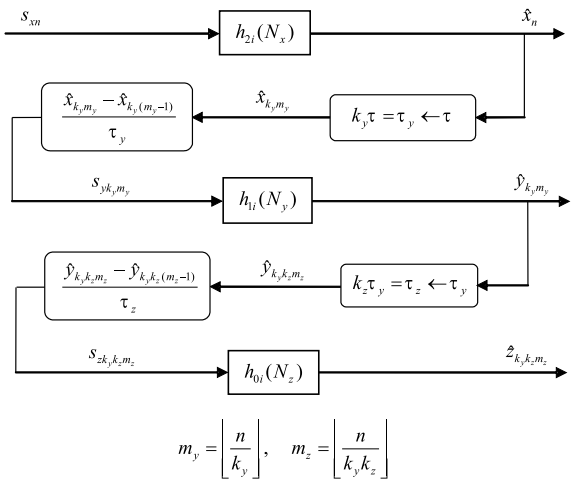

Figure 8: The thinning FIR filtering algorithm for TIE measurements of the 3-state clock model.

measurement of the second state is artificially formed by the backward time derivative as

$$s_{yk_y m_y} = \frac{\hat{x}_{k_y m_y} - \hat{x}_{k_y(m_y-1)}}{k_y \tau} . \tag{75}$$

The estimate $\hat{y}_{k_y m_y}$ of the second state is then provided at each $k_y m_y$ point in a like manner using the gain h_{1i} to yield

$$\hat{y}_{k_y m_y} = \sum_{i=0}^{N_y-1} h_{1i} s_{yk_y(m_y-1)} . \tag{76}$$

Similarly, the estimate $\hat{z}_{k_y k_z m_z}$ can be found and two particular cases recognized.

3-state clock model. For the clock identified to have three states, the thinning unbiased FIR filtering algorithm results in the following batch forms:

$$\hat{x}_n = \sum_{i=0}^{N_x-1} h_{2i} s_{n-i} , \tag{77}$$

$$\hat{y}_{k_y m_y} = \frac{1}{k_y \tau} \sum_{j=0}^{N_y-1} h_{1i} [\hat{x}_{k_y(m_y-j)} - \hat{x}_{k_y(m_y-j-1)}] , \tag{78}$$

$$\hat{z}_{k_y k_z m_z} = \sum_{r=0}^{N_z-1} \frac{\hat{y}_{k_y k_z(m_z-r)} - \hat{y}_{k_y k_z(m_z-r-1)}}{k_y k_z \tau N_z} . \tag{79}$$

It can be shown that the first correct estimate of the third state, for the worst case of asynchronous thinning, appears at $N_x - 1 + k_y(N_y + k_z N_z)$.

2-state clock model. The 2-state model fits well atomic clocks and is often applied to crystal clocks. For this model, the thinning algorithm is given by

$$\hat{x}_n = \sum_{i=0}^{N_x-1} h_{1i} s_{n-i}\,, \tag{80}$$

$$\hat{y}_{k_y m_y} = \frac{1}{k_y \tau N_y} \sum_{j=0}^{N_y-1} [\hat{x}_{k_y(m_y-j)} - \hat{x}_{k_y(m_y-j-1)}]\,. \tag{81}$$

In the worst case of asynchronous thinning, the first correct estimate of the second state appears at $N_x - 1 + k_y N_y$.

Applications of both basic and thinning algorithms to crystal clocks can be found in [22, 23, 24, 25, 27, 28, 30].

8.3 Generic p-shift Optimal Estimation Algorithm

Assigned the $K \times N$ gain matrix $\mathbf{H}(p)$, the estimate $\tilde{\mathbf{x}}_{n+p} = \mathbf{H}(p)\mathbf{S}_{n,m}$ of the clock state $\mathbf{x}_n$ has been found in [21] at $n + p$ as

$$\tilde{\mathbf{x}}_{n+p} = \bar{\mathbf{H}}(p)\mathbf{Z}_m(\mathbf{Z}_m + \tilde{\mathbf{Z}}_\Psi + \mathbf{\Phi}_V)^{-1}\mathbf{S}_{n,m} \tag{82}$$

$$= \mathbf{A}^{n-m+p}(\mathbf{C}_{n-m}^T\mathbf{C}_{n-m})^{-1}\mathbf{C}_{n-m}^T \times \mathbf{Z}_m(\mathbf{Z}_m + \tilde{\mathbf{Z}}_\Psi + \mathbf{\Phi}_V)^{-1}\mathbf{S}_{n,m}\,, \tag{83}$$

where $\mathbf{Z}_m$ is determined by solving the discrete algebraic Riccati equation (DARE)

$$\mathbf{0} = \mathbf{Z}_m(\tilde{\mathbf{Z}}_\Psi + \mathbf{\Phi}_V)^{-1}\mathbf{Z}_m + 2\mathbf{Z}_m + \tilde{\mathbf{Z}}_\Psi + \mathbf{\Phi}_V - \mathbf{S}_{n,m}\mathbf{S}_{n,m}^T(\tilde{\mathbf{Z}}_\Psi + \mathbf{\Phi}_V)^{-1}\mathbf{Z}_m\,, \tag{84}$$

and

$$\bar{\mathbf{H}}(p) = \mathbf{A}^{n-m+p}(\mathbf{C}_{n-m}^T\mathbf{C}_{n-m})^{-1}\mathbf{C}_{n-m}^T \tag{85}$$

is the unbiased gain associated with the noiseless both system and measurement when $\tilde{\mathbf{Z}}_\Psi = \mathbf{0}$ and $\mathbf{\Phi}_V = \mathbf{0}$. Table 1 summarizes the generic p-shift optimal FIR estimation algorithm of the clock state at $n + p$.

8.4 Generic recursive p-shift Unbiased Estimation Algorithm

The unbiased FIR estimate of clock state has been found in [21] in the batch form of

$$\tilde{\mathbf{x}}_{n+p|n} = \bar{\mathbf{H}}(p)\mathbf{S}_{n,m} \tag{86}$$

$$= \mathbf{A}^{n-m+p}(\mathbf{C}_{n-m}^T\mathbf{C}_{n-m})^{-1}\mathbf{C}_{n-m}^T\mathbf{S}_{n,m} \tag{87}$$

Table 1: Generic p-Shift Optimal FIR Estimation Algorithm

Stage	
Given:	$N \geqslant K$ and p
Set:	$\bar{\mathbf{H}}(p) = \mathbf{A}^{N-1+p}(\mathbf{C}_{N-1}^T\mathbf{C}_{N-1})^{-1}\mathbf{C}_{N-1}^T$
Find $\mathbf{Z}_{n-N+1}$:	$\mathbf{0} = \mathbf{Z}_{n-N+1}(\tilde{\mathbf{Z}}_\Psi + \mathbf{\Phi}_V)^{-1}\mathbf{Z}_{n-N+1} + 2\mathbf{Z}_{n-N+1} + \tilde{\mathbf{Z}}_\Psi + \mathbf{\Phi}_V$ $-\mathbf{S}_{n,n-N+1}\mathbf{S}_{n,n-N+1}^T(\tilde{\mathbf{Z}}_\Psi + \mathbf{\Phi}_V)^{-1}\mathbf{Z}_{n-N+1}$
Compute:	$\tilde{\mathbf{H}}_n(p) = \bar{\mathbf{H}}(p)\mathbf{Z}_{n-N+1}(\mathbf{Z}_{n-N+1} + \tilde{\mathbf{Z}}_\Psi + \mathbf{\Phi}_V)^{-1}$
	$\tilde{\mathbf{x}}_{n+p} = \tilde{\mathbf{H}}_n(p)\mathbf{S}_{n,n-N+1}$

Table 2: Recursive Form of the Generic p-Shift Unbiased FIR Estimation Algorithm

Stage	
Given:	K, N, p, $v = K, ..., N-1$
Set:	$\mathbf{\Xi} = \mathbf{A}^T\mathbf{C}^T\mathbf{C}\mathbf{A}$
	$\mathbf{P}_{K-1} = (\mathbf{C}_{K-1}^T\mathbf{C}_{K-1})^{-1}$
	$\mathbf{F}_{K-1} = \mathbf{A}^{K-1}\mathbf{P}_{K-1}(\mathbf{A}^{K-1})^T$
	$\tilde{\mathbf{x}}_{n-N+K+p} = \mathbf{A}^{K-1+p}\mathbf{P}_{K-1}{\mathbf{C}_{K-1}}^T\mathbf{S}_{n-N+K,n-N+1}$
Update:	$\mathbf{F}_v = \mathbf{A}\mathbf{F}_{v-1}\mathbf{A}^T - \mathbf{A}\mathbf{F}_{v-1}(\mathbf{I} + \mathbf{\Xi}\mathbf{F}_{v-1})^{-1}\mathbf{\Xi}\mathbf{F}_{v-1}\mathbf{A}^T$
	$\tilde{\mathbf{x}}_{n-N+1+v+p} = \mathbf{A}\tilde{\mathbf{x}}_{n-N+v+p} + \mathbf{A}^p\mathbf{F}_v\mathbf{C}^T(s_{n-N+1+v} - \mathbf{C}\mathbf{A}^{1-p}\tilde{\mathbf{x}}_{n-N+v+p})$
Instruction:	Use $\tilde{\mathbf{x}}_{n-N+1+v+p}$ as the output when $v = N-1$

and in the recursive form given in Table 2. Here, a set of auxiliary functions, $\mathbf{\Xi}$, $\mathbf{P}_{K-1}$, and $\mathbf{F}_{K-1}$, is computed and *a posteriori* initial vector $\tilde{\mathbf{x}}_{n-N+K+p}$ determined via measurement without prediction. Then an auxiliary matrix $\mathbf{F}_v$ and the estimate vector $\tilde{\mathbf{x}}_{n-N+1+v+p}$ are both updated by changing v from K to $N-1$ for all $n \geqslant K$. The true estimate is taken when $v = N-1$.

Note that both algorithms (Table 1 and Table 2) can be used on arbitrary averaging horizons. If all the data available is employed, from zero to n, one must set $m = n - N + 1 = 0$.

9 The Trade-off with the Kalman Algorithm

The Kalman-Bucy algorithm [12] is useful for various applications in timescales [7]. However, it is known to be a nice engineering solution if the noise sources are all white sequences and there are no uncertainties neither in the model nor in the measurement. Otherwise, the algorithm may become noisy and unstable [8, 13, 14].

Contrary to the infinite impulse response (IIR) recursive structures, including the Kalman-Bucy filter, the transversal FIR ones demonstrate the following important properties [11, 13, 14, 26]:

- Inherent BIBO stability featured to weighted average.
- Better robustness against temporary uncertainties and round-off errors, especially when $N \gg 1$.
- Convergence of optimal and unbiased estimates with $N \gg 1$.

Experimental and numerical evidences of these advantages can be found in many papers [8, 13, 14, 22, 29, 30]. As an example, Fig. 9 sketches typical errors featured to the 2-degree (ramp) optimal FIR filter and two-state Kalman filter [29], both applied to the GPS-based measurement of a crystal clock imbedded in the Stanford Frequency Counter SR620. As can be seen, there is no time delay between the estimates and the filters thus have similar time constants. Herewith, the FIR filter demonstrates better robustness against the GPS time uncertainty, producing lower noise and smaller regular errors.

10 Applications

Below, we observe several most typical applications of FIR filtering to GPS-based timekeeping. For a comparison, the relevant Kalman estimates are also discussed. The results have been obtained using a measurement set (Fig. 1) with the GPS timing SynPaQ III Sensor as a receiver, Stanford Frequency Counter SR625, and local crystal clock imbedded in the SR625. Actual clock errors have been measured simultaneously for the Symmetricom cesium standard of frequency CsIII.

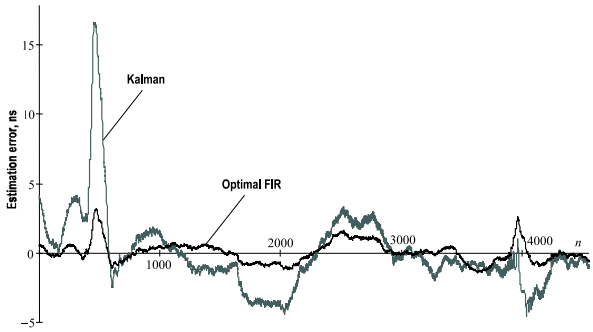

Figure 9: Typical errors in the GPS-based TIE filtering estimates produced by the 2-degree optimal FIR filter and two-state Kalman filter [29].

10.1 Estimation of the TIE

Figure 10a sketches a typical GPS-based measurement with sawtooth (for about 2 hours) and an actual TIE behavior. It also incorporates the unbiased FIR estimate $\hat{x}_n$ and the Kalman estimate $\hat{x}_{Kn}$ [30].

To ascertain the difference between the estimates, Fig. 10b shows the time deviation (TDEV) [5, 6] computed over all the measurement points. As can be seen, the TDEV associated with $\hat{x}_n$ and $\hat{x}_{Kn}$ behave closely to each other and trace above the actual values. Although, better behavior of the FIR estimate can be watched.

10.2 Estimation of the Frequency Offset

In [30], the thinning algorithm (79) has been applied in order to estimate the second clock state. Following [24], the minimum MSE in the FIR estimate was found in the range of $10s \leqslant \tau \leqslant 100s$ and the filter parameters were allowed to be $k_y = 100$ and $N_y = 130$.

Figure 11 shows the GPS-based and reference measurements along with the FIR and Kalman estimates. One infers from Fig. 11a that both $\hat{x}_2$ and $\hat{x}_{2K}$ fit well the actual trend (reference measurement) and the time derivative of the thinned out estimate of the TIE (GPS-measurement). The goodness-of-fit estimates are demonstrated in Fig. 11b in terms of the Allan deviation (ADEV) [5]. One notices that the FIR filter produces much lower noise that the Kalman filter when $\tau < 10^3$ s, although both estimates still inherently trace above the actual value.

10.3 Clock Steering

Steering of the local clock errors in the loop (Fig. 1) has been investigated in [3]. Because only fast noise components are commonly filtered out in clock

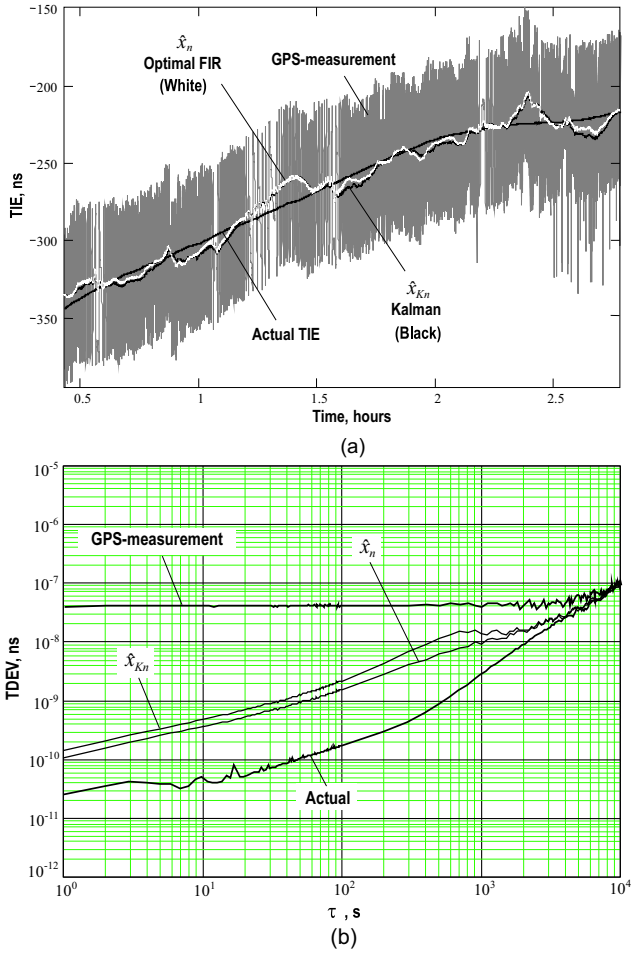

Figure 10: Typical GPS-based measurement with sawtooth and estimates of the TIE of a crystal clock [30]: (a) measurements and estimates and (b) TDEV.

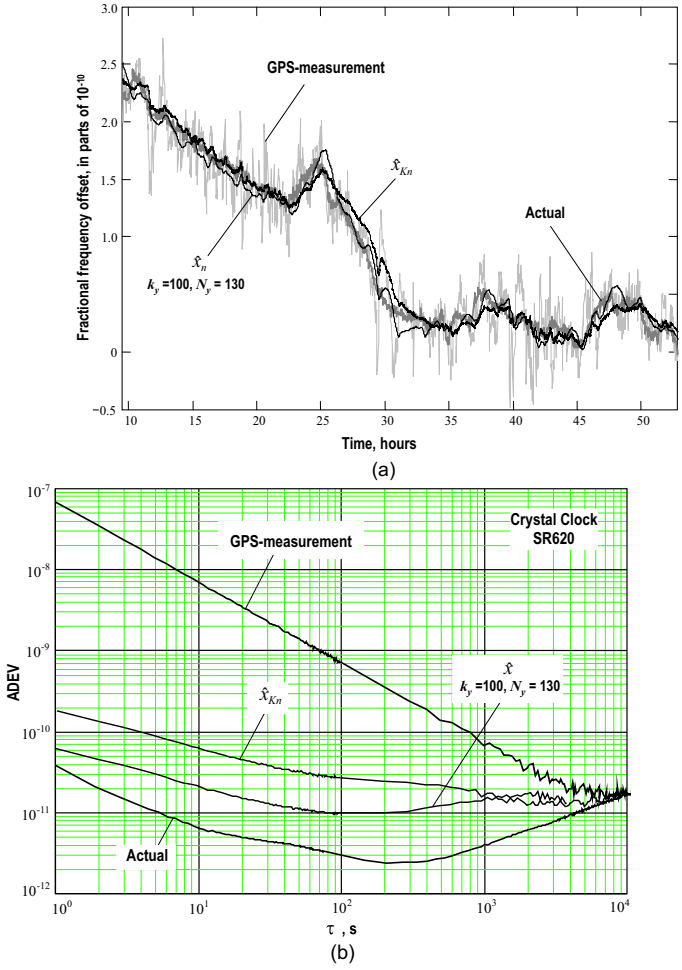

Figure 11: Typical GPS-based measurement with sawtooth and estimates of the fractional frequency offset of a crystal clock [30]: (a) measurements and estimates and (b) ADEV.

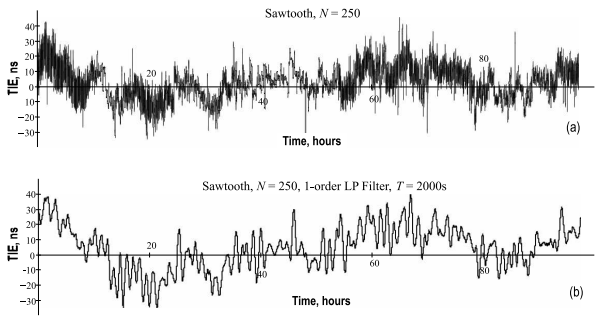

Figure 12: Typical errors in the GPS-based TIE filtering estimates produced by the 2-degree optimal FIR filter and two-state Kalman filter [29].

synchronization, an averaging horizon was chosen as shown in Fig. 2 ("Filtering of the TIE behavior") to produce a minimum MSE in the output of a GPS-locked crystal clock.

For the GPS-based measurement with sawtooth, the optimum N was experimentally found, as in [24], to be $N_{\text{opt}} \cong 250$. By this value, the TIE has been measured to range from -30 ns to 40 ns over time as shown in Fig. 12a. An additional 1-order low-pass (LP) filter included to the loop with the time constant $T = 2000$ s was used for smoothing the TIE as shown in Fig. 12b.

As can be seen, the smoothed TIE (Fig. 12b) ranges within the same bounds as in the origin (Fig. 12a). Therefore, a subtle comparison of both function was provided in [3] in terms of the TDEV and ADEV (Fig. 13).

The TDEV of the unlocked crystal clock inherently increases with large averaging time, whereas the reference GPS 1PPS signal with sawtooth has a uniform TDEV function (Fig. 13a). The optimal FIR filter included to the loop allows for a substantial steering of clock errors with large averaging times. An additional smoothing filter (1-order LP with $T = 1000$ s) completes the picture, providing a substantial noise reduction for small averaging times. It can be seen that the resulting TDEV traces much lower the mask specified in [6] for digital communications networks.

Contrary to the TDEV, the ADEV of the reference GPS 1PPS signal decreases linearly in the Bode plot, whereas that of the unlocked crystal clock inherently reduces and then grows passing through a minimum (Fig. 13b). The effect of the optimal FIR filter with the smoothing 1-order LP filter included in the loop results in the following. In the locked crystal clock, noise with small averaging times mostly depends on precision of its oscillator (effect of the smoothing filter) and time error departures with large averaging times are limited by the accuracy of the optimal FIR filter output. Note that an excursion in the ADEV observed in the middle of the averaging times range shown in Fig. 13 cannot be avoided from the standpoint of control. Its peak value can only be minimized and position optimized by the smoothing filter.

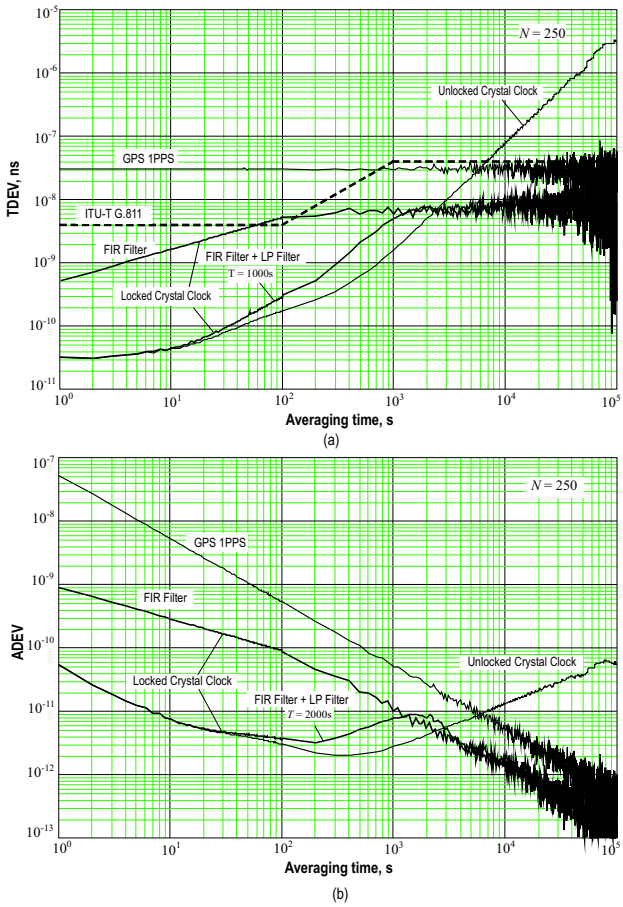

Figure 13: Typical errors of the GPS-locked crystal clock [3]: (a) TDEV and (b) ADEV.

11 Conclusions

In this paper, we observed recent advantages in GPS-based estimation and steering of local clock errors employing FIR algorithms. Advantages of the approach against the Kalman filter were shown experimentally for real measurements in the presence of the GPS temporary time uncertainty and non Gaussian sawtooth noise induced by the GPS timing receiver.

Both the optimal and unbiased FIR solutions can be used in order to estimate clock state with minimum errors via the GPS-based measurement. An important point here is that simple unbiased polynomial FIR estimators with gains (24)–(26) become virtually optimal at large averaging horizons, $N \gg 1$, featured to clock problems. That means, by extension, that unbiased FIR estimators (filters, predictors, and smoothers) with such gains may become the best choice in terms of simplicity, accuracy, stability, and robustness for GPS-based timekeeping. First of all, it relates to GPS-based clock estimation and synchronization. Such estimators can also be useful in design of the GNSS composed clock algorithms, in which case any increase in accuracy is highly appreciated.

12 Acknowledgements

The first author would like to thank Dr. Demetrios Matsakis of the United States Naval Observatory (USNO) for the offer to give a Tutorial at the V Int. Time Scale Algorithms Symp. (San Fernando, Spain, 28–30 April, 2008), to Dr. Judah Levine of the National Institute of Standards and Technology (NIST) for the invitation to give a Tutorial at the joint meeting of the IEEE Int. Freq. Control Symp. and European Freq. Time Forum (Besançon, France, 20–24 April, 2009), to Prof. Nikos Mastorakis of the Technical University of Sofia for the invitation to give a Plenary Lecture at the WSEAS 1st Int. Conf. on Computational and Information Science (Houston, 30 April–2 May, 2009), and to Prof. Nasser Kehtarnavaz of the University of Texas at Dallas for the invitation to give a seminar at the Dallas Section of the IEEE Signal Processing Society (Dallas, 19 October, 2009).

References

[1] Allan DW, Ashby N, Hodge CC. The Science of Timekeeping. Application Note 1289. Hewlett Packard: Englewood, CO, 1997; 1-88.

[2] Allan DW, Barnes JA. Optimal time and frequency transfer using GPS signals. Proceedings of 36th Annual Frequency Control Symposium, Philadelphia, PA, June 1982; 378-87.

[3] Arceo-Miquel L, Shmaliy YS, Ibarra-Manzano O. Optimal synchronization of local clocks by GPS 1PPS signals using predictive FIR filters. IEEE Trans Inst Meas 2009; 58: 1833-40.

[4] Chaffee JW. Relating the Allan variance to the diffusion coefficients of a linear stochastic diferential equation model for precision oscillators. IEEE Transactions on Ultrasonics, Ferroelectr Freq Control 1987; 34: 655-58.

[5] IEEE Standard 1139. Standard definitions of physical quantities for fundamental frequency and time metrology- random instabilities 1999.

[6] ITU-T Recommendation G.811. Timing characteristics of primary reference clocks 1997.

[7] Galleani L, Tavella P. On the use of the Kalman filter in timescales. Metrologia 2003; 40: 326-34.

[8] Fitzgerald RJ. Divergence of the Kalman filter. IEEE Trans Automat Contr 1971; AC-16: 736-47.

[9] Heinonen P, Neuvo Y. FIR-median hybrid filters with predictive FIR structures. IEEE Trans Acoust 1988; 36: 892-99.

[10] Hwang SY, Minimum uncorrelated unit noise in state-space digital filtering. IEEE Trans Acoust 1977; 25: 273-281.

[11] Jazwinski AH. Stochastic Processes and Filtering Theory. New York: Academic Press 1970.

[12] Kalman RE, Bucy RS. New results in linear filtering and prediction theory. ASME J Bas Eng 1961; 83D: 95-108.

[13] Kwon WH, Kim PS, Han SH. A receding horizon unbiased FIR filter for discrete-time state space models. Automatica 2002; 38: 545-51.

[14] Kwon WH, Kim PS, Park P. A receding horizon Kalman FIR filter for discrete time-invariant systems. IEEE Trans Automat Contr l999; 44: 1787-91.

[15] Lepek A. Clock prediction and characterization. Metrologia 1997; 34: 379-86.

[16] Lewandowski W, Petit G, and Thomas C. Precision and accuracy of GPS time transfer. IEEE Trans Inst and Meas1993; 42: 474-79.

[17] McBurney PW, Woo AN, Rode F. System and method for frequency management in a communication device having a positioning feature. US Patent 7598909, 2009.

[18] Meyer F. Common-view and melting-pot GPS time transfer with the UT+. Proceedings of the 32nd Annual PTTI Meeting, Reston, VA, November 2004; 147-56.

[19] Nakagawa M. Low power GPS receiver system and method of using same. US Patent 7529157, 2009.

[20] Park BJ, Lim CS. Track model constraint for GPS position. US Patent 7446701, 2008.

[21] Shmaliy YS. GPS-Based Optimal FIR Filtering of Clock Models. New York: Nova Science Pub 2009.

[22] Shmaliy YS. An unbiased FIR filter for TIE model of a local clock in applications to GPS-based timekeeping. IEEE Trans Ultrason Ferroelectr Freq Control 2006; 53: 862-70.

[23] Shmaliy YS. A simple optimally unbiased MA filter for timekeeping. IEEE Trans Ultrason Ferroelectr Freq Control 2002; 49: 789-97.

[24] Shmaliy YS, Muñoz-Diaz J, Arceo-Miquel L. Optimal horizons for a one parameter family of unbiased FIR filters. Digital Signal Process 2008; 18: 739-50.

[25] Shmaliy YS, Ibarra-Manzano O. Optimal FIR filtering of the clock time errors. Metrologia 2008; 45: 571-76.

[26] Shmaliy YS. On real-time optimal FIR estimation of linear TIE models of local clocks. IEEE Trans Ultrason Ferroelectr Freq Control 2007; 54: 2403-06.

[27] Shmaliy YS, Arceo-Miquel L. Effective predictive estimator for holdover in GPS-based clock synchronization. IEEE Trans Ultrason Ferroelectr Freq Control 2008; 55: 2131-39.

[28] Shmaliy YS. An unbiased p-step predictive FIR filter for a class of noise free discrete-time models with independently observed states. Signal, Image and Video Process 2009; 3: 127-35.

[29] Shmaliy YS. Optimal gains of FIR estimators for a class of discrete-time state-space models. IEEE Signal Process Lett 2008; 15: 517-20.

[30] Shmaliy YS, Ibarra-Manzano O, Arceo-Miquel L, Muñoz-Diaz J. A thinning algorithm for GPS-based unbiased FIR estimation of a clock TIE model. Measurement 2008; 41: 538-50.

[31] Shmaliy YS. Unbiased FIR filtering of discrete-time polynomial state-space models. IEEE Trans Signal Process 2009; 57: 1241-49.

[32] Smith SW. The Scientist and Engineer's Guide to Digital Signal Processing. 2nd Ed. San Diego: California Technical Publishing1997.

[33] Stark H, Woods JW. Probability, Random Processes, and Estimation Theory for Engineers, 2nd Ed. New Jersey: Prentice Hall 1994.

[34] Wang C-S, Xiong L, Jia Z, Dong L, Liv J. Timing calibration for fast signal reacquisition in navigational receivers. US Patent 7456782, 2008.

[35] Woz B. Synchronization of an external device using a GPS receiver. US Patent 7460955, 2008.

[36] Zhou X, Wang X. FIR-median hybrid filters with polynomial fitting. Digital Signal Process 2004; 14: 112-24.

Received: November 11, 2009 Revised: December 1, 2009 Accepted: December 7, 2009